

# InAs/InGaAsP Quantum Dots Emitting at 1.5 $\mu\text{m}$ for Applications in Lasers

E.S. Semenova<sup>1,\*</sup>, I.V. Kulkova<sup>1</sup>, S. Kadkhodazadeh<sup>1,2</sup>, M. Schubert<sup>1</sup>, R.E. Dunin-Borkowski<sup>2</sup>, K. Yvind<sup>1</sup>

<sup>1</sup> DTU Fotonik, Technical University of Denmark, 2800 Kgs. Lyngby, Denmark

<sup>2</sup> DTU Center for Electron Nanoscopy, Technical University of Denmark, 2800 Kgs. Lyngby, Denmark

\* esem@fotonik.dtu.dk

## Abstract

In this work the epitaxial growth of InAs quantum dots (QDs) in an InGaAsP matrix on an InP wafer is described. A new approach to shift the emission wavelength to the 1.5 $\mu\text{m}$  region using deposition of a thin GaAs capping layer on top of the QDs is suggested and exploited. Laser structures based on 5 layers of such dots as the gain material demonstrate lasing in continuous wave regime at 1.5  $\mu\text{m}$  wavelength at room temperature.

## 1 Introduction

The unique density of states and associated carrier dynamic properties [1] of quantum dots (QDs) make them highly interesting for ultrafast optical devices, in particular as a gain medium for mode-locked lasers [2, 3]. So far, most work has been done on the InAs/GaAs material system (e.g. [4, 5, 6]). However, in order to be compatible with photonic integration, InAs/InGaAsP/InP QDs operating at 1.55  $\mu\text{m}$  optical wavelength are required.

Due to the smaller lattice mismatch of InAs/InP in comparison to InAs/GaAs, the size of the resulting QDs is significantly larger, leading to an emission wavelength above 1.7  $\mu\text{m}$ . Therefore, different approaches have been applied to shift the emission from QDs to the 1.5  $\mu\text{m}$  wavelength range, such as double capping growth [7] or a GaAs underlayer [8].

The work presented here aims to develop a growth process for defect free InAs/InGaAsP QDs operating at a wavelength of 1.5  $\mu\text{m}$  that is suitable as gain material for mode-locked lasers. QDs are grown by metal organic vapour phase epitaxy (MOVPE) and their optical and morphological properties are characterized. Finally, continuous wave (CW) lasing in ridge waveguide laser structures of those QDs is demonstrated.

## 2 Experiments

The studied structures were grown by low pressure MOVPE (Discovery 125) on a (001) InP substrate at 76 Torr. Hydrogen was used as a carrier gas and standard precursors (trimethylindium, trimethylgallium, arsine, phosphine and tertiarybutylphosphine) were used as growth sources. The wafer temperature during growth was monitored in real time by an emissivity-corrected pyrometer and was 610 $^{\circ}\text{C}$  for the deposition of InP and InGaAsP layers and 515 $^{\circ}\text{C}$  for QD deposition and deposition of the following 10 nm thick InGaAsP capping layer. V/III ratio was reduced from  $\sim 200$  down to 5 for the QD formation. Two types of epitaxial structures were grown. The first set of structures was used for optical and structural analysis and consisted of 40 nm thick InGaAsP layer ( $Q_{1.08}$ , which means that this layer is lattice matched to the InP substrate and has a room temperature bandgap corresponding to 1.08  $\mu\text{m}$ ) with an array of InAs QDs grown in the middle. In order to obtain an emission wavelength of around 1.5  $\mu\text{m}$ , we applied the following QD fabrication procedure: 1.65 ML InAs QDs were deposited on top of  $Q_{1.08}$ , then, after 5 second growth interruption under arsine, capped with 1.7 ML GaAs and then an InGaAsP capping layer. The second type of structure grown was a laser structure. The active region consisted of five layers of InAs/GaAs QDs (described above) in a 450 nm thick InGaAsP ( $Q_{1.08}$ ) waveguide, which was sandwiched between n- and p-doped InP cladding layers.

To study the shape, size and chemical composition of the QDs and the GaAs capping layer, high resolution scanning transmission electron microscopy (STEM) in plan-view and cross-sectional geometries was used. Photoluminescence (PL) measurements with different excitation power and wavelength in the temperature range 64-300 K were used to investigate the optical properties of the QDs.

### 3 Results and discussion

#### 3.1. Structural characterization

Due to the fact that the lattice mismatch in the InAs-InP material system is half as much as that in the InAs-GaAs system, the QDs formed in the first case have larger volumes. The amount of deposited InAs (effective thickness) of QDs was chosen to be 1.65 ML, which is very close to the critical thickness for QD formation in this material system. In this way we ensured that the QDs formed were as small as possible. However, the QDs obtained also exhibit a broad size distribution. Figure 1 shows a plan-view high-angle annular dark-field (HAADF) STEM image of an array of InAs/InGaAsP QDs. The QDs appear as bright regions, as the image intensity in HAADF STEM images is strongly dependent on atomic number.

These QDs do not show a significant elongation and appear as multi-faceted structures with hexagonal bases. The QDs in this sample have a number density of  $4 \cdot 10^{10} \text{ cm}^{-2}$ , an average base length of  $31.9 \pm 2 \text{ nm}$  and an average height of about 2.6 nm.

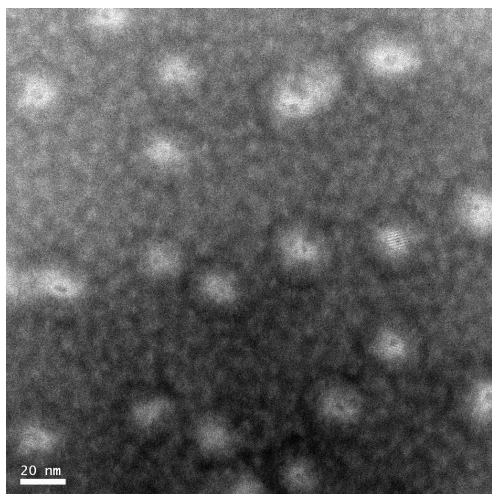


**Figure 1** Plan-view HAADF STEM image of an array of 1.65 ML InAs QDs grown on InGaAsP and covered with a 1.7 ML GaAs layer, prior to full capping with InGaAsP.

To study the influence of the GaAs capping layer on the growth dynamics, the morphology and chemical

composition of the QDs and the surrounding material were examined using high-resolution STEM and energy-dispersive X-ray spectroscopy (EDS). In order to simplify the data analysis, the QDs were deposited inside an InP matrix instead of InGaAsP. It was found that deposition of a thin GaAs capping layer of 1.5-1.7ML thickness leads to a decrease in the heights of the QDs. The InAs removed from the tops of the QDs forms an InGaAs alloy with GaAs and segregates around the bases of the QDs (forming InGaAs “rings” surrounding the perimeters of the QDs). The resulting QDs are shallow and have flat tops. More details of these studies are described in [9]. Our optical measurements confirm that the same process takes place in the InAs-InGaAsP structures, where the same blue shift of the central emission wavelength with increasing GaAs thickness was observed.

#### 3.2. Optical characterization.

The capping of the QDs with a thin GaAs layer results in a strong blue-shift of the emission wavelength of the QDs. Shown in figure 2 are room temperature PL spectra for QDs covered with 0 ML, 1.5 ML and 1.7 ML of GaAs. QDs which are not covered with GaAs have their PL peak maxima above  $1.7 \mu\text{m}$ , whereas with increasing thickness of the GaAs capping the corresponding PL peaks are strongly blue shifted. A GaAs capping thickness of 1.7 ML shifts the QD spectrum to the desired wavelength of  $1.53 \mu\text{m}$ .

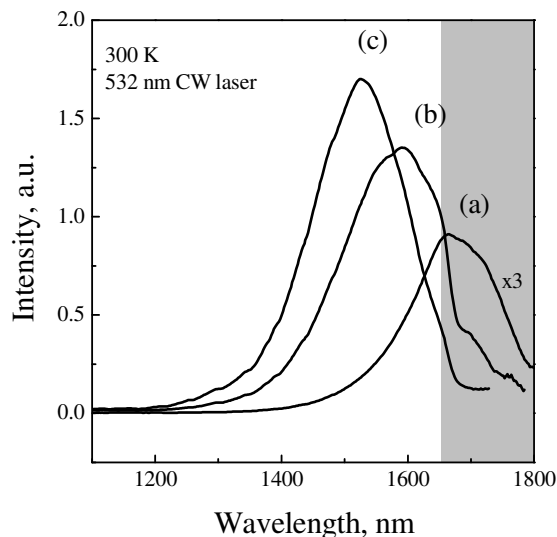


**Figure 2** Room temperature PL spectra of InAs QDs in an InGaAsP ( $Q_{1.08}$ ) matrix for different GaAs capping layer thicknesses: (a) no GaAs, (b) 1.5 ML GaAs, (c) 1.7 ML GaAs. The grey area shows the sensitivity cut-off of the detector.

The uniformity of the PL peak maximum across the 2" wafer is approximately 10 nm and the PL full width at half maximum (FWHM) is 170 nm, which is an evidence of the broad size distribution of the QDs.

Shown in figure 3 is the PL spectrum of InAs QDs covered with 1.7 ML of GaAs, taken at 64 K. The spectrum contains a modulation with multiple peaks. Such a modulation is associated with multi-modal dot ensemble formation, where the height of the QDs changes in increments of 1 ML (As mentioned before, these QDs are shallow and have flat tops). According to a kinetic model of multimodal QD ensemble evolution [10], the QD growth kinetic is largely controlled by stress, which is concentrated at the base perimeters of the dots. The QDs have a truncated pyramidal shape. For every base size there is an optimal height, which is higher for larger bases. Thus, different lines in the PL spectrum shown in figure 3 correspond to QDs with one monolayer height difference. The same QD behaviour as in our case has been described and systematically studied in [10, 11] for InAs QDs in GaAs. The modulation of the PL spectrum described above can also be seen in the electroluminescence spectra.

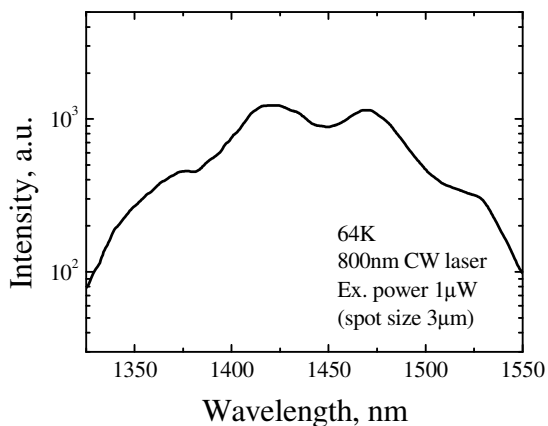


**Figure 3** PL spectrum of InAs QDs covered with 1.7 ML of GaAs taken at 64 K.

The ratio between the integrated QD PL intensities at 64 K and room temperature, taken with the same optical excitation power, is approximately 3. This number confirms the good optical properties of the QDs presented here and shows that there are almost no centers of non-radiative recombination.

**3.3. Laser performance.**

In order to test the performance of the QDs described above, we implemented them as the gain material in a laser.

The epitaxial material containing 5 QD layers in the active region was processed into ~2 µm ridge waveguide devices using BCB (Cyclotene 3046) planarization. Ni/Ge/Au and Ti/Pt/Au contacts were deposited onto the

n- and p- doped sides, respectively, and the devices were soldered epi-side up to AlN heatsinks [12]. No facet coatings were deposited.

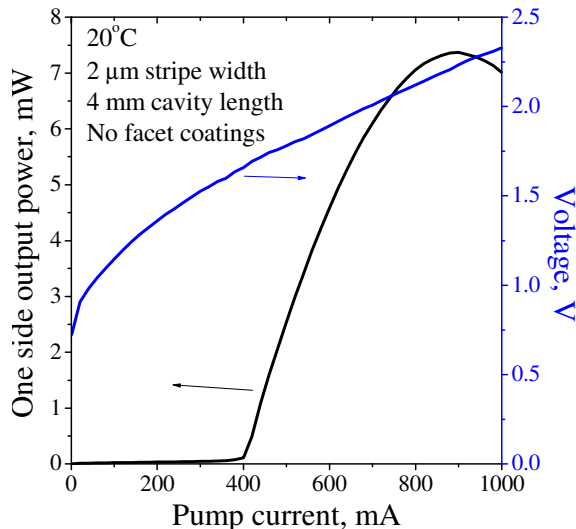


**Figure 4** CW light-current (black) and voltage-current (blue) characteristic of a 2 µm wide stripe QD laser (L = 4 mm) at 20°C heat sink temperature

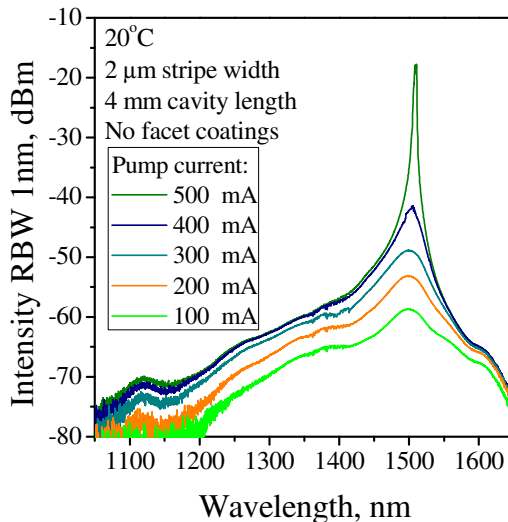


**Figure 5** EL and CW lasing spectra of a 2 µm wide stripe QD laser (L = 4 mm) at 20°C heat sink temperature.

The devices were measured in continuous wave (CW) regime at room temperature. In figure 4 the light-current (black) and voltage-current (blue) characteristics are shown for a cavity length of 4 mm. The threshold current is ~400 mA for 4 mm long devices (and ~275 mA for 2 mm long devices). The maximum output power for the 4 mm cavity length device is about 7.4 mW. With further increasing of the pump current the optical output power

drops, which is due to heating of the active region and has a reversible behaviour.

The corresponding electroluminescence and CW lasing spectra are presented in figure 5 for different drive currents. Lasing occurs at the desired wavelength of  $\sim 1.5 \mu\text{m}$ . We attribute the wide spectral bandwidth as the main reason for the rather high threshold current seen, since all QDs with different sizes are pumped but only one type of QDs with a certain height and thus emission wavelength contribute to the lasing process. All injected carriers contribute to the device losses which, combined with the low gain, results in reduced efficiency of this generation of devices. While mode-locked lasers, which are the ultimate goal of this study, do need a wide spectral bandwidth, we anticipate that a reduced spectral bandwidth will probably be optimal for the currently achievable pulse widths.

## 4 Conclusion

The present work describes metal organic vapour phase epitaxy of InAs/InGaAsP quantum dots with an emission wavelength around  $1.5 \mu\text{m}$ . The proposed and demonstrated method describes the deposition of QDs with an effective thickness close to the critical thickness for QD formation, and following capping with thin GaAs layer. GaAs layer deposition results in the redistribution of QD material, resulting in shallow dots with flat top, which in its turn results in a strong blue-shift of the emission wavelength to the desired  $1.5 \mu\text{m}$  wavelength region.

This QD ensemble is described by a large size distribution. Of prime importance is the height fluctuation of shallow QDs in increments of 1 ML. This fluctuation results in modulation of the PL spectrum at low temperature and of the electroluminescence spectra of the laser structure.

The QDs were applied as a gain material in a laser structure and demonstrate lasing in the continuous wave regime at room temperature from narrow ridge waveguide devices with different cavity lengths.

The wide spectral bandwidth, due to the QD size distribution, while good for mode-locking, does lower the efficiency of these devices. However, the emission from waveguide layers with only a factor of 3 reduction of integrated PL between 64K and 300K indicate good optical and crystalline quality.

## Acknowledgments:

The authors gratefully acknowledge financial support from the Danish Research Council under the research programs Optical Sampling for Coherent Detection Receivers (OPSCODER), QUantum dot structures Enabling light Slow-down and amplificaTion (QUEST), Femtosecond semiconductor lasers harnessed (FLASH) and the Villum Kann Rasmussen center of excellence NATEC. ESS thanks the European Commission for funding through the Marie Curie Incoming International Fellowship (project number 252890). The authors thank Per Lunnemann Hansen for fruitful discussions.

## 5 Literature

- 1 A. Markus, J. X. Chen, C. Paranthoën, A. Fiore, C. Platz, O. Gauthier-Lafaye, *Appl. Phys. Lett* **82** (12), 1818 (2003)
- 2 K. Yvind D. Larsson, J. Mørk, J. M. Hvam, M. Thompson, R. Penty, I. White. Photonics West 2008, paper 6909, pp 69090A1-9 (2008)
- <sup>3</sup> T. Akiyama, M. Sugawara, Y. Arakawa, Proceedings of the IEEE, Vol. 95, No. 9, 1757 (2007).
- 4 M. Kuntz, G. Fiol, M. Laemmlin, C. Meuer, D. Bimberg, Proceedings of the IEEE, **95**, No. 9, 1767, (2007)
- 5 M. G. Thompson, A. R. Rae, Mo Xia, R. V. Penty, I. H. White, IEEE Journal of Selected Topics in Quantum Electronics, **15**, No. 3, ( 2009)
- 6 E. U. Rafailov, M. A. Cataluna, W. Sibbett, Nature Photonics **1**, 395–401 (2007).
- 7 Z.G. Lu Z.G. Lu, J.R. Liu, P.J. Poole, S. Raymond, P.J. Barrios, D. Poitras, G. Pakulski, P. Grant, and D. Roy-Guay Optics Express **17** pp 13609–13614 (2009)
- 8 S. Anantathanasarn *et al.*, J. Crystal Growth, **298** pp. 553–557 (2007)
- 9 S. Kadkhodazadeh, E. S. Semenova, K. Yvind and R. E. Dunin-Borkowski, to be published
- 10 U. W. Pohl, K. Pötschke, A. Schliwa, F. Guffarth, D. Bimberg N. D. Zakharov, P. Werner M. B. Lifshits and V. A. Shchukin, D. E. Jesson, PHYSICAL REVIEW B **72**, 245332 (2005)
- 11 R. Heitz, F. Guffarth, K. Pötschke, A. Schliwa, D. Bimberg N. D. Zakharov, P. Werner, PHYSICAL REVIEW B **71**, 045325 (2005)
- 12 K. Yvind, D. Larsson, L. J. Christiansen, C. Angelo, L. K. Oxenløwe, J. Mørk, D. Birkedal, J. M. Hvam, and J. Hanberg. Photonics Technology Letters, **16** (4): 975-977, (2004)